

## Effects of small interfering RNA inhibit Class I phosphoinositide 3-kinase on human gastric cancer cells

Bao-Song Zhu, Li-Yan Yu, Kui Zhao, Yong-You Wu, Xiao-Li Cheng, Yong Wu, Feng-Yun Zhong, Wei Gong, Qiang Chen, Chun-Gen Xing

Bao-Song Zhu, Li-Yan Yu, Kui Zhao, Yong-You Wu, Yong Wu, Feng-Yun Zhong, Wei Gong, Qiang Chen, Chun-Gen Xing, Department of General Surgery, The Second Affiliated Hospital, Soochow University, Suzhou 215004, Jiangsu Province, China

Xiao-Li Cheng, Department of Gastroenterology, Qianfoshan Hospital, Shandong University, Jinan 250014, Shandong Province, China

**Author contributions:** Xing CG and Zhu BS designed the research; Xing CG, Zhu BS, and Zhao K wrote the paper; Zhao K and Yu LY collected and analyzed data; Zhu BS, Wu YY, Zhong FY, and Cheng XL selected the color figures in the paper; all authors contributed to the intellectual context and approved the final version of the manuscript.

**Supported by** The Natural Science Foundation of China, No. 81172348; Suzhou High-Level Talents Project, 2008-11; Suzhou Science and Technology Development Foundation, 2010SYS201031; and the Science, Education, and Health Foundation of Suzhou City, SWKQ0914 and SWKQ0916

**Correspondence to:** Chun-Gen Xing, Professor, Department of General Surgery, The Second Affiliated Hospital of Soochow University, 1055 San Xiang Road, Suzhou 215004, Jiangsu Province, China. xingcg@126.com

Telephone: +86-512-67784106 Fax: +86-512-67784106

Received: April 5, 2012 Revised: September 19, 2012

Accepted: December 25, 2012

Published online: March 21, 2013

### Abstract

**AIM:** To investigate the effects of small interfering RNA (siRNA)-mediated inhibition of Class I phosphoinositide 3-kinase (Class I PI3K) signal transduction on the proliferation, apoptosis, and autophagy of gastric cancer SGC7901 and MGC803 cells.

**METHODS:** We constructed the recombinant replication adenovirus PI3K(I)-RNA interference (RNAi)-green fluorescent protein (GFP) and control adenovirus NC-RNAi-GFP, and infected it into human gastric cancer cells. MTT assay was used to determine the growth rate

of the gastric cancer cells. Activation of autophagy was monitored with monodansylcadaverine (MDC) staining after adenovirus PI3K(I)-RNAi-GFP and control adenovirus NC-RNAi-GFP treatment. Immunofluorescence staining was used to detect the expression of microtubule-associated protein 1 light chain 3 (LC3). Mitochondrial membrane potential was measured using the fluorescent probe JC-1. The expression of autophagy was monitored with MDC, LC3 staining, and transmission electron microscopy. Western blotting was used to detect p53, Beclin-1, Bcl-2, and LC3 protein expression in the culture supernatant.

**RESULTS:** The viability of gastric cancer cells was inhibited after siRNA targeting to the Class I PI3K blocked Class I PI3K signal pathway. MTT assays revealed that, after SGC7901 cancer cells were treated with adenovirus PI3K(I)-RNAi-GFP, the rate of inhibition reached 27.48%  $\pm$  2.71% at 24 h, 41.92%  $\pm$  2.02% at 48 h, and 50.85%  $\pm$  0.91% at 72 h. After MGC803 cancer cells were treated with adenovirus PI3K(I)-RNAi-GFP, the rate of inhibition reached 24.39%  $\pm$  0.93% at 24 h, 47.00%  $\pm$  0.87% at 48 h, and 70.30%  $\pm$  0.86% at 72 h ( $P < 0.05$  compared to control group). It was determined that when 50 MOI, the transfection efficiency was 95%  $\pm$  2.4%. Adenovirus PI3K(I)-RNAi-GFP (50 MOI) induced mitochondrial dysfunction and activated cell apoptosis in SGC7901 cells, and the results described here prove that RNAi of Class I PI3K induced apoptosis in SGC7901 cells. The results showed that adenovirus PI3K(I)-RNAi-GFP transfection induced punctate distribution of LC3 immunoreactivity, indicating increased formation of autophagosomes. The results showed that the basal level of Beclin-1 and LC3 protein in SGC7901 cells was low. After incubating with adenovirus PI3K(I)-RNAi-GFP (50 MOI), Beclin-1, LC3, and p53 protein expression was significantly increased from 24 to 72 h. We also found that Bcl-2 protein expression down-regulated with the treatment of adenovirus PI3K(I)-RNAi-GFP (50 MOI). A number of

isolated membranes, possibly derived from ribosome-free endoplasmic reticulum, were seen. These isolated membranes were elongated and curved to engulf a cytoplasmic fraction and organelles. We used transmission electron microscopy to identify ultrastructural changes in SGC7901 cells after adenovirus PI3K(I)-RNAi-GFP (50 MOI) treatment. Control cells showed a round shape and contained normal-looking organelles, nucleus, and chromatin, while adenovirus PI3K(I)-RNAi-GFP (50 MOI)-treated cells exhibited the typical signs of autophagy.

**CONCLUSION:** After the Class I PI3K signaling pathway has been blocked by siRNA, the proliferation of cells was inhibited and the apoptosis of gastric cancer cells was enhanced.

© 2013 Baishideng. All rights reserved.

**Key words:** Gastric cancer cells; Class I phosphoinositide 3-kinase; RNA interference; Apoptosis; Autophagy

Zhu BS, Yu LY, Zhao K, Wu YY, Cheng XL, Wu Y, Zhong FY, Gong W, Chen Q, Xing CG. Effects of small interfering RNA inhibit Class I phosphoinositide 3-kinase on human gastric cancer cells. *World J Gastroenterol* 2013; 19(11): 1760-1769 Available from: URL: <http://www.wjgnet.com/1007-9327/full/v19/i11/1760.htm> DOI: <http://dx.doi.org/10.3748/wjg.v19.i11.1760>

## INTRODUCTION

Gastric cancer is the fourth most common cancer and the second leading cause of cancer death worldwide<sup>[1]</sup>, with nearly a million new cases diagnosed each year. The phosphatidylinositol 3-kinases (PI3Ks) are a family of lipid kinases whose primary biochemical function is to phosphorylate the 3-hydroxyl group of phosphoinositides<sup>[2]</sup>. Phosphorylation results in the activation of second messenger molecules, with consequent signal transduction that sets in motion a variety of physiological cellular metabolic and survival functions.

The PI3K-serine/threonine kinase (AKT)-mammalian target of the rapamycin (mTOR) pathway is an important cellular pathway involved in cell growth, tumorigenesis, cell invasion, and drug response<sup>[3-5]</sup>. This pathway is frequently activated in many cancers, and uncontrolled PI3K-AKT-mTOR signaling may also result in poor clinical outcome in lung, cervical, ovarian, and esophageal cancers<sup>[3,4,6-8]</sup>.

PI3Ks are grouped into three Classes (I-III), with varying structure and substrate preference. The functions of Class I PI3Ks relate to glucose homeostasis, metabolism, growth, proliferation, and survival. Isoform-specific roles are described, albeit with degrees of overlap, with potential implications for toxicity and efficacy of novel inhibitors of Class I PI3Ks<sup>[9]</sup>. A substantial body of evidence exists in support of the notion that not only does PI3K pathway activation promote cell survival and tumor

progression, but also can predict for therapeutic resistance to a broad range of anticancer therapies.

The discovery of Class I PI3K revealed a novel role for autophagy in induced cell death, and Class I PI3K is believed to be a crucial modulator in both apoptosis and autophagy. Our aim was to detect the effects of adenovirus PI3K(I)-RNA interference (RNAi)-green fluorescent protein (GFP) on the growth and apoptosis of gastric cancer cells *in vitro*. To compare transduction efficiency, biological and molecular mechanisms of adenovirus PI3K(I)-RNAi-GFP on gastric cancer cell lines will be detected.

## MATERIALS AND METHODS

### Reagents

SGC7901 and MGC801 gastric cancer cells were purchased from the Shanghai Institute of Cell Biology, Chinese Academy of Sciences (Shanghai, China). RPMI1640 medium was purchased from Gibco (Rockville, MD, United States). Fetal bovine serum was obtained from Hangzhou Sijiqing Biological Engineering Material Co., Ltd. (Hangzhou, China), L-glutamine and MTT were provided by Sigma (St Louis, MO, United States). Antibodies against p53, Bcl-2, Beclin-1, and LC3 were provided by Cell Signaling Technology (Beverly, MA, United States).

### Adenoviral vectors and infections

RNAi sequence design against Class I PI3K and the construction of vectors expressing Class I PI3K short hairpin RNA (shRNA). The Class I PI3K-specific target sequence was chosen according to online shRNA tools of Invitrogen (<http://www.invitrogen.com/rnai>) using the Class I PI3K reference sequence (GenBank accession No. NM\_006218). The target sequence was designed as follows: Class I PI3K (base 3090-3118), "5'-AGAG-GTTTCAGGAGATGTGTT ACAAG GCT-3'". shRNAs were then chemically synthesized and a lentiviral vector was constructed. The exact insertion of the specific shRNA was further confirmed by sequencing. The recombinant adenovirus vector that expresses shRNA against Class I PI3K was synthesized by Shanghai Genesil Co., Ltd. Stocks of replication-defective adenoviral vectors expressing green fluorescent protein [adenovirus PI3K(I)-RNAi-GFP and control adenovirus NC-RNAi-GFP] were stored at -80 °C. Infections were performed at 70% to 75% confluence in DMEM supplemented with 2% FCS. Cells were subsequently incubated at 37 °C for at least 4 h, followed by the addition of fresh medium. Cells were subjected to functional analyses at fixed time points following infection as described for individual experimental conditions.

### Determination of optimal multiplicity of infection

$1 \times 10^4$  SGC7901 and MGC803 cells/well were seeded in 96 well plates to 60%-70% cultured adherent cells. Different multiplicities of infection (MOI = 10, 20, 30,

50, 100) of the adenovirus NC-RNAi-GFP (100  $\mu$ L) and diluted infected cells were then added. Eight hours later, 10% fetal bovine serum for RPMI1640 culture medium was added, and 48 h later was counted under a fluorescence microscope to calculate the number of cells that expressed GFP.

### Cell culture and viability assay

SGC7901 and MGC803 cells were maintained in RPMI1640 medium containing 10% heat-inactivated fetal bovine serum and 0.03% *L*-glutamine incubated in a 5% CO<sub>2</sub> atmosphere at 37 °C. Cells in a mid-log phase were used in experiments. Cell viability was assessed by MTT assay. To determine the response of SGC7901 cells to adenovirus PI3K(I)-RNAi-GFP, SGC7901 cells were plated into 96-well microplates ( $7 \times 10^4$  cells/well) and adenovirus PI3K(I)-RNAi-GFP was added to a culture medium and cell viability was assessed with MTT assay 24 h after adenovirus PI3K(I)-RNAi-GFP treatment. MTT (Sigma, St Louis, MO, United States) solution was added to a culture medium (500 mg/L final concentration) for 4 h before the end of treatment, and the reaction was stopped by the addition of 10% acidic SDS (100  $\mu$ L). The absorbance value (*A*) at 570 nm was read using an automatic multiwell spectrophotometer (Bio-Rad, Richmond, CA, United States). The percentage of cell proliferation was calculated as follows: cell proliferation (%) =  $(1 - A \text{ of experiment well} / A \text{ of positive control well}) \times 100\%$ .

### Visualization of monodansylcadaverine-labeled vacuoles

Exponentially-growing cells were plated onto 24-chamber culture slides, cultured for 24 h, and then incubated with the drug in 10% FCS/RPMI 1640 for 12 and 24 h. Autophagic vacuoles were labeled with MDC<sup>[10]</sup> (Sigma, St Louis, MO, United States) by incubating cells with 0.001 mmol/L MDC in RPMI1640 at 37 °C for 10 min. After incubation, cells were washed three times with phosphate-buffered saline (PBS) and immediately analyzed with a fluorescence microscopy (Nikon Eclipse TE 300, Japan) equipped with a filter system (V-2A excitation filter: 380-420 nm, barrier filter: 450 nm). Images were captured with a CCD camera and imported into Photoshop.

### Immunofluorescence staining LC3

MGC803 cells were seeded onto 24-chamber culture slides and treated with adenovirus PI3K(I)-RNAi-GFP (50 MOI) and adenovirus NC-RNAi-GFP. After fixation in methanol for 10 min and blocked with a buffer containing 1% bovine serum albumin (BSA) and 0.1% Triton X-100 for 1 h, cells were incubated with either the primary antibody against LC3 from Cell Signaling Technology (Beverly, MA, United States) or diluted at 1:200 with PBS containing 1% BSA at 4 °C overnight. Cells were then incubated for 1 h with 1:500 secondary fluorescence conjugated antibodies (Sigma) to visualize the binding sites of the primary antibody under a laser confocal microscope

(Leisa, Germany).

### Detection of mitochondrial potential

Mitochondrial  $\Delta\psi$  was determined using the KeyGEN Mitochondrial Membrane Sensor Kit (KeyGEN, Nanjing, China). The MitoSensor dye aggregates in the mitochondria of healthy cells and emits red fluorescence against green monomeric cytoplasmic background staining. However, in cells with a collapsed mitochondrial  $\Delta\psi$ , the dye cannot accumulate in the mitochondria and remains as monomers throughout the cells with green fluorescence<sup>[11]</sup>. SGC7901 cells were briefly incubated with adenovirus PI3K(I)-RNAi-GFP in 24-well plates for the indicated times, then pelleted, washed with PBS, and resuspended in 0.5 mL of diluted MitoSensor reagent (1 mmol/L in incubation buffer). After incubating cells with MitoSensor reagent for 20 min, 0.2 mL of incubation buffer was added and cells were centrifuged then resuspended in 40  $\mu$ L of incubation buffer. Finally, cells were washed and resuspended in 1 mL PBS for flow cytometry analysis.

### Total cell protein extraction and Western blotting analysis

For extraction of total cell proteins, cells were washed with pre-cooled PBS and subsequently lysed in pre-cooled RIPA lysis buffer (50 mmol Tris-HCl, pH 7.4, 150 mmol NaCl, 1 mmol dithiothreitol, 0.25% sodium deoxycholate, and 0.1% NP-40) containing 1 mmol/L phenylmethylsulfonyl fluoride, 50 mmol sodium pyrophosphate, 1 mmol/L Na<sub>3</sub>VO<sub>4</sub>, 1 mmol NaF, 5 mmol EDTA, 5 mmol EGTA, and a protease inhibitors cocktail. Cell lysis was performed on ice for 30 min. Clear protein extracts were obtained by centrifugation for 30 min at 4 °C. Protein extraction from SGC7901 gastric cancer cells was performed as previously described. Protein concentration was determined with a Bradford protein assay kit. Proteins were resolved on 8.5% polyacrylamide gels and subsequently transferred onto nitrocellulose membranes. For immunoblotting, nitrocellulose membranes were incubated with specific antibodies recognizing target proteins overnight at 4 °C. The membranes were then incubated with horseradish peroxidase-conjugated secondary antibody (1:3000) for 1 h at room temperature, and subsequently analyzed by an enhanced chemiluminescence detection system (Amersham Pharmacia Biotech) and visualized by autoradiography. Protein  $\beta$ -actin (1:5000; Sigma) was used as a loading control.

### Transmission electron microscopic examination

Pursuant to treatment with adenovirus PI3K(I)-RNAi-GFP, cells were fixed in ice-cold 2.5% glutaraldehyde in 0.1 mol/L PBS, and preserved at 4 °C for further processing. When processing resumed, cells were post-fixed in 1% osmium tetroxide in the same buffer, dehydrated in graded alcohols, embedded in Epon 812, sectioned with an ultra-microtome, and stained with uranyl acetate and lead citrate, followed by examination with a transmission

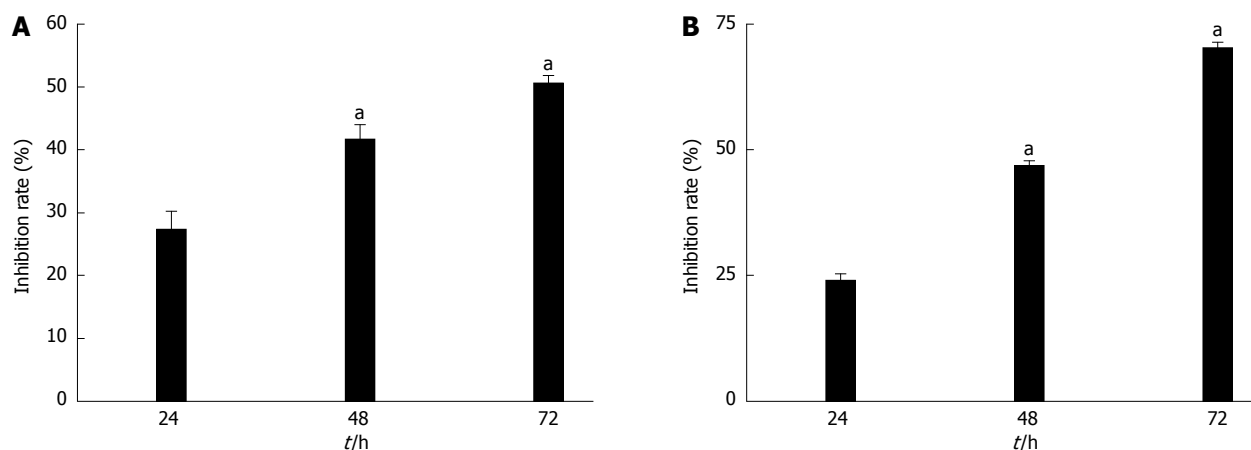


**Figure 1** Reduced viability of SGC7901 and MGC803 cells after adenovirus Class I phosphoinositide 3-kinase-RNA interference-green fluorescent protein treatment. A: SGC7901 cells ( $7 \times 10^4$  cells/mL); B: MGC803 cells ( $7 \times 10^4$  cells/mL) cultured with adenovirus Class I phosphoinositide 3-kinase [PI3K(I)]-RNA interference-green fluorescent protein (RNAi-GFP) (50 MOI) and adenovirus negative control-RNAi-GFP for 24, 48, and 72 h. Cell viability was analyzed by MTT assay. Values were given as mean  $\pm$  SD of three independent experiments. <sup>a</sup> $P < 0.05$  vs control group.

electron microscope (Philips CM120, Dutch).

### Statistical analysis

All data were presented as mean  $\pm$  SD. Statistical analysis was carried out by ANOVA, followed by a Dennett's-test, with  $P < 0.05$  being considered significant.

## RESULTS

### Cell viability was detected after adenovirus PI3K(I)-RNAi-GFP treatment

MTT assay showed that the inhibition rate of gastric cancer cells transfected with adenovirus PI3K(I)-RNAi-GFP was significantly higher than adenovirus NC-RNAi-GFP (50 MOI) ( $P < 0.05$ ). Adenovirus PI3K(I)-RNAi-GFP inhibited the proliferation of SGC7901 and MGC803 cancer cell viability. MTT assays revealed that, after 24 h of treatment with adenovirus PI3K(I)-RNAi-GFP, the rate of inhibition for SGC7901 cancer cells had reached  $27.48\% \pm 2.71\%$ . The rate of inhibition rose when the incubation time was prolonged, reaching  $41.92\% \pm 2.02\%$  at 48 h, and  $50.85\% \pm 0.91\%$  at 72 h after treatment (Figure 1). It was also revealed that, after 24 h of treatment with adenovirus PI3K(I)-RNAi-GFP, the rate of inhibition for MGC803 cancer cells had reached  $24.39\% \pm 0.93\%$ . The rate of inhibition rose when the incubation time was prolonged, reaching  $47.00\% \pm 0.87\%$  at 48 h, and  $70.30\% \pm 0.86\%$  at 72 h after treatment (Figure 1).

### Transfection efficiency and cell morphology were detected by fluorescence microscope

With the treatment of adenovirus PI3K(I)-RNAi-GFP (50 MOI) transfected SGC7901 and MGC803 cells after 24 h, we found that the cell body was swollen and rounded, with the cells showing further deformation after 48 h. For fragments of recombinant adenovirus containing GFP, after transfection with 72 h, SGC7901 and MGC803 cells can be counted under a fluorescence

microscope due to the green fluorescence of the tumor cells (Figure 2). It was determined that when 50 MOI, the transfection efficiency was  $95\% \pm 2.4\%$ .

### Adenovirus PI3K(I)-RNAi-GFP transfection increased autophagic vacuoles:

The autofluorescent substance MDC has been recently shown to be a marker for late autophagic vacuoles (L-AVs), but not endosomes<sup>[10]</sup>. The dye is trapped in acidic, membrane-rich organelles, and also exhibits increased fluorescence quantum yield in response to the compacted lipid bilayers present in L-AVs<sup>[12]</sup>. When cells are viewed with a fluorescence microscope, AVs stained by MDC appear as distinct dot-like structures distributed within the cytoplasm or localizing in the perinuclear regions. We found that there was an increase in the number of MDC-labeled vesicles after treatment of adenovirus PI3K(I)-RNAi-GFP (50 MOI) from 24 to 72 h (Figure 3).

### Adenovirus PI3K(I)-RNAi-GFP transfection increased punctate LC3:

Microtubule-associated protein 1 light chain 3 (LC3), the mammalian ontology of Atg8, targets to the autophagosomal membranes in an Atg5-dependent manner and remains there even after Atg12-Atg5 dissociates. LC3 is considered to be the only credible marker of the autophagosome in mammalian cells<sup>[13]</sup>. We used immunofluorescence staining to detect the expression and localization of LC3. The results showed that adenovirus PI3K(I)-RNAi-GFP transfection induced punctate distribution of LC3 immunoreactivity, indicating an increased formation of autophagosomes by adenovirus PI3K(I)-RNAi-GFP (Figure 4).

### Adenovirus PI3K(I)-RNAi-GFP transfection induced mitochondrial dysfunction:

In the present study, mitochondrial membrane potential was examined using the fluorescent dye JC-1. We detected a collapse in mitochondrial membrane potential ( $\Delta\psi$ ) as early as 24 h after adenovirus PI3K(I)-RNAi-GFP (50 MOI) treatment, as indicated by the increased emission of green fluorescence.

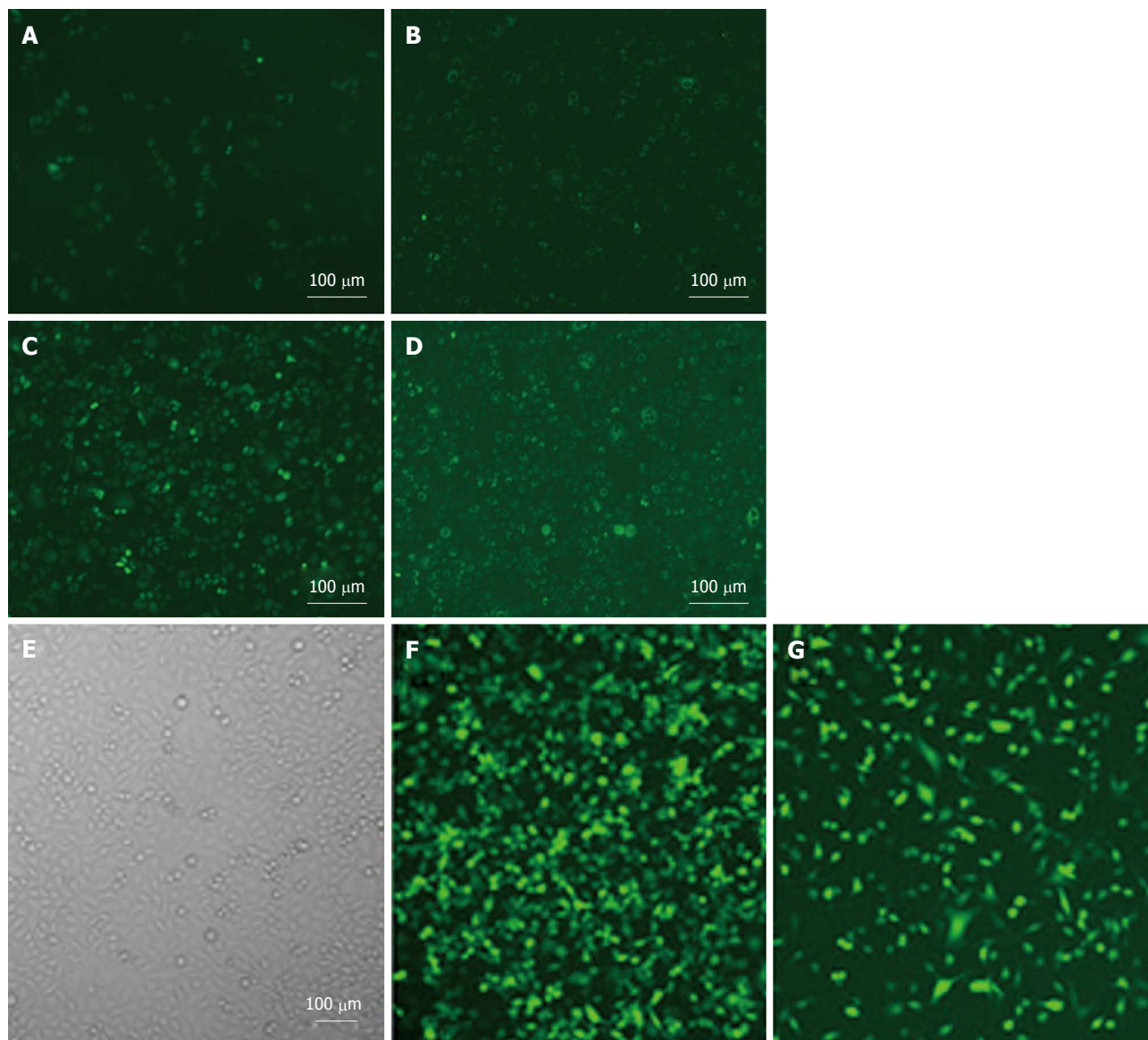


**Figure 2** Transfection efficiency and cell morphology were detected by fluorescence microscope after adenovirus Class I phosphoinositide 3-kinase-RNA interference-green fluorescent protein and adenovirus negative control-RNA interference-green fluorescent protein treatment. A-D: SGC7901 cells; E-G: MGC803 cells incubated with adenovirus Class I phosphoinositide 3-kinase [PI3K(I)]-RNA interference-green fluorescent protein (RNAi-GFP) (50 MOI) for the indicated time. A and E: Control group; B and F: 24 h after adenovirus PI3K(I)-RNAi-GFP treatment; C and G: 48 h adenovirus PI3K(I)-RNAi-GFP (50 MOI) treatment; D: 72 h after adenovirus PI3K(I)-RNAi-GFP (50 MOI) treatment ( $\times 200$ ) ( $n = 3$ ).

This change reached its maximum at 24 h after adenovirus PI3K(I)-RNAi-GFP (50 MOI) treatment (Figure 5). A collapse in mitochondrial membrane potential always indicates cell apoptosis or necrosis. Adenovirus PI3K(I)-RNAi-GFP (50 MOI) induced mitochondrial dysfunction and activated cell apoptosis in SGC7901 cells, and the results described here prove that RNAi of Class I PI3K induced apoptosis in SGC7901 cells.

**Adenovirus PI3K(I)-RNAi-GFP transfection up-regulated the expression of Beclin-1 and LC3:** To assay if adenovirus PI3K(I)-RNAi-GFP (50 MOI) transfection increases the expression of autophagic relative protein, Western blotting analysis was used to detect the expression of LC3 and Beclin-1. The results showed that the

basal level of Beclin-1 and LC3 protein in SGC7901 cells was low. After incubating with adenovirus PI3K(I)-RNAi-GFP(50 MOI), Beclin-1 and LC3 protein expression was significantly increased from 24 to 72 h (Figure 6).

**Adenovirus PI3K(I)-RNAi-GFP transfection increased the expression of p53 and decreased the expression of Bcl-2:** To assay if adenovirus PI3K(I)-RNAi-GFP (50 MOI) transfection influences the expression of apoptotic relative protein, Western blotting analysis was used to detect the expression of Bcl-2 and p53. The results showed that the basal level of p53 protein in SGC7901 cells was low. After incubating with adenovirus PI3K(I)-RNAi-GFP, p53 protein expression was significantly increased from 24 to 72 h. We found that Bcl-2 protein expression down-regulated

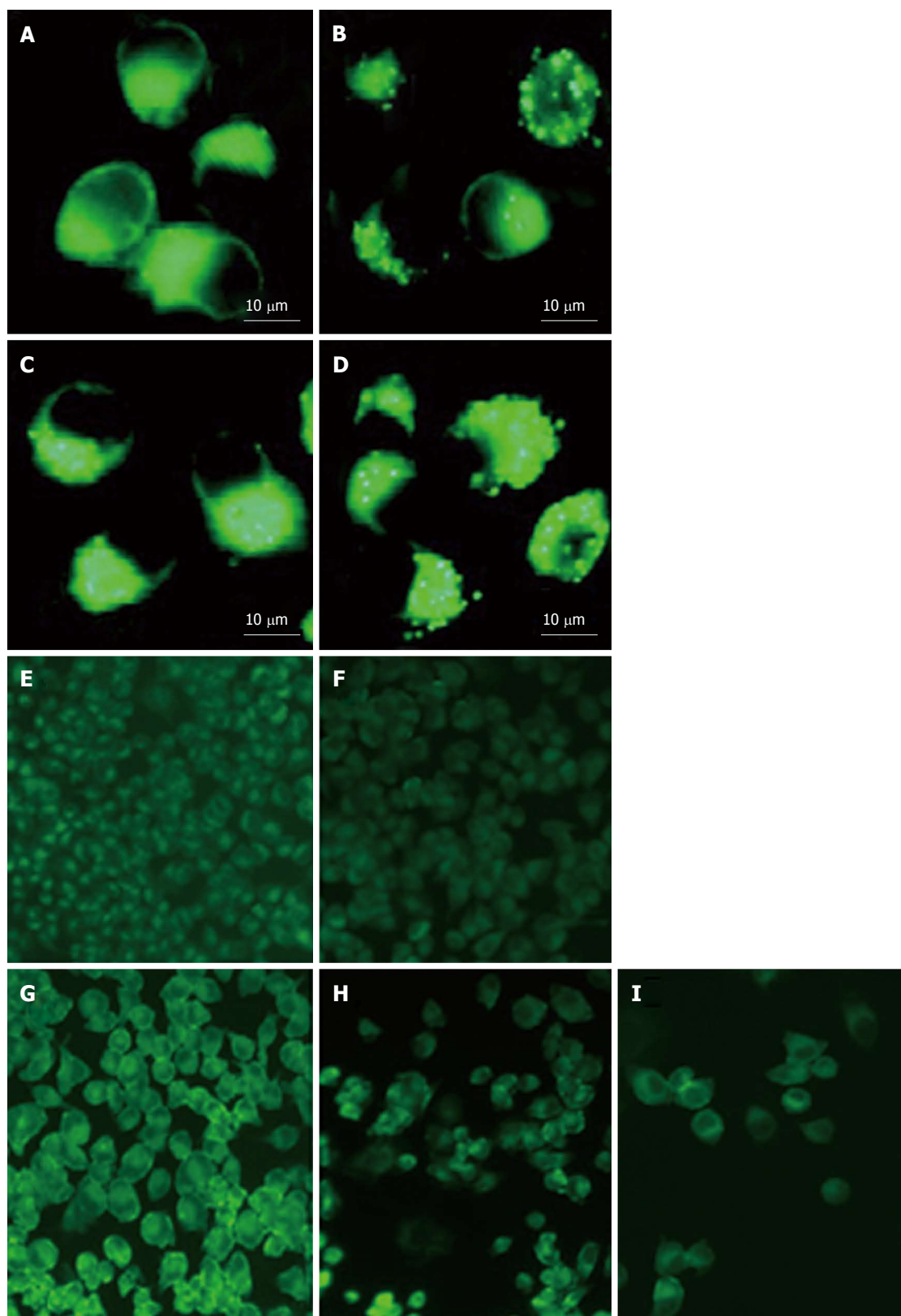


**Figure 3** Monodansylcadaverine staining showed autophagy was activated after adenovirus Class I phosphoinositide 3-kinase-RNA interference-green fluorescent protein (50 MOI) treatment. A-D: SGC7901 cells; E-I: MGC803 cells incubated with adenovirus Class I phosphoinositide 3-kinase [PI3K(I)]-RNA interference-green fluorescent protein (RNAi-GFP) (50 MOI) and adenovirus negative control (NC)-RNAi-GFP for the indicated time and stained with monodansylcadaverine (100  $\mu\text{mol/L}$ ). Fluorescence particles showed L-acoustic vector sensor. A and E: Control; B and F: Adenovirus NC-RNAi-GFP; C and G: 24 h after adenovirus PI3K(I)-RNAi-GFP (50 MOI) treatment ( $\times 200$ ) ( $n = 3$ ); D and H: 48 h after adenovirus PI3K(I)-RNAi-GFP (50 MOI) treatment; I: 72 h after adenovirus PI3K(I)-RNAi-GFP (50 MOI) treatment ( $\times 1000$ ) ( $n = 3$ ).

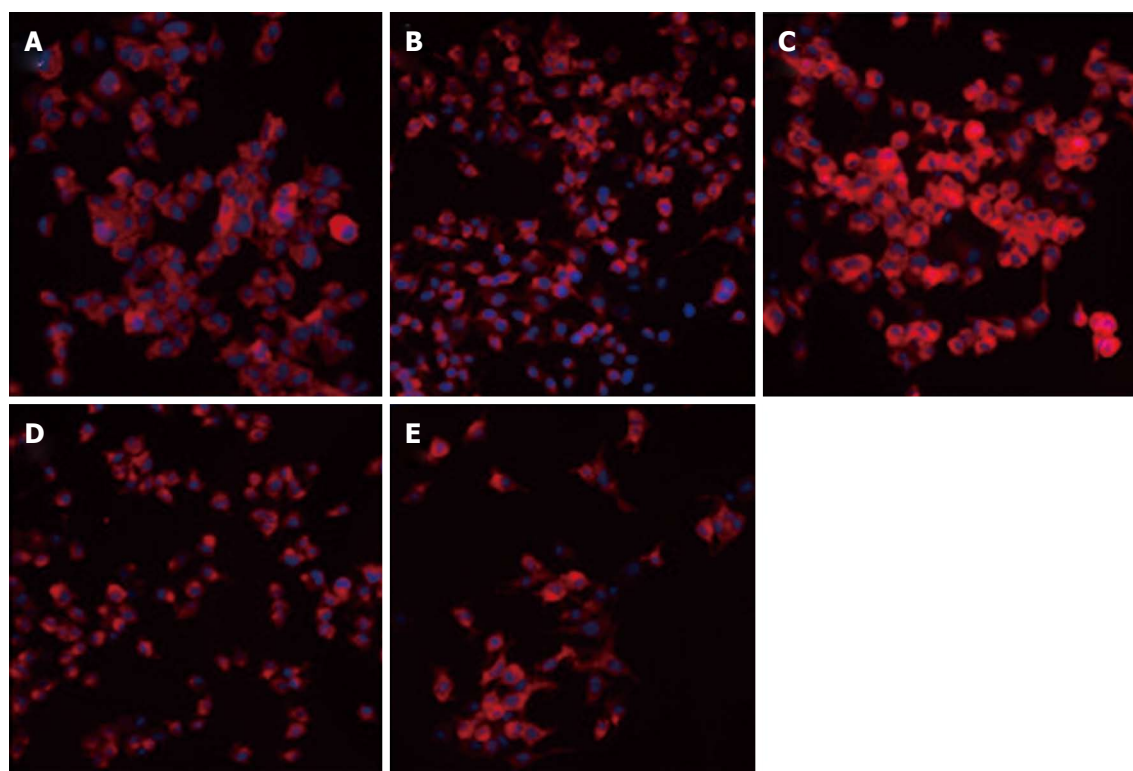


**Figure 4** Microtubule-associated protein 1 light chain 3 expression and location in MGC803 cells after treatment with adenovirus Class I phosphoinositide 3-kinase-RNA interference-green fluorescent protein. Cells were treated with adenovirus Class I phosphoinositide 3-kinase [PI3K(I)]-RNA interference-green fluorescent protein (RNAi-GFP) (50 MOI) for 24 h (C), 48 h (D), and 72 h (E), and analyzed with an immunofluorescence microscope. A: Control; B: Adenovirus negative control-RNAi-GFP ( $\times 400$ ) ( $n = 3$ ). Adenovirus PI3K(I)-RNAi-GFP increased the punctate distribution of light chain 3 from 24 to 72 h.

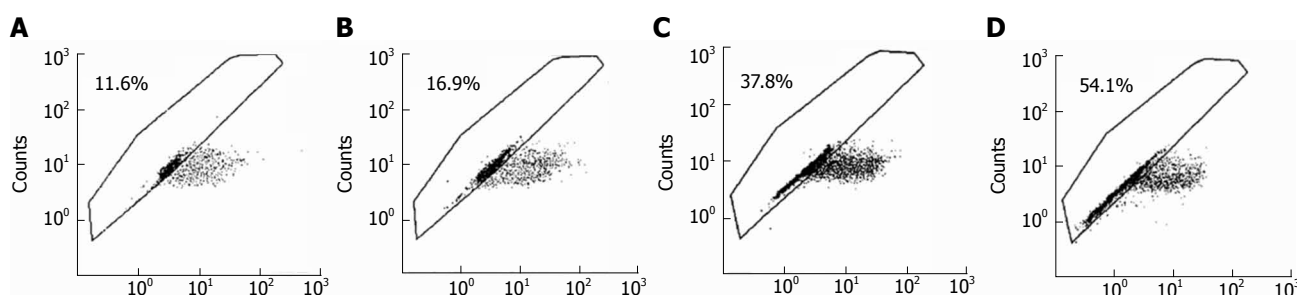


**Figure 5** Flow cytometric analysis of mitochondria membrane potential in the control and adenovirus Class I phosphoinositide 3-kinase-RNA interference-green fluorescent protein-treated SGC7901 cells. A: Control: adenovirus negative control RNA interference-green fluorescent protein (RNAi-GFP), cells were treated with adenovirus Class I phosphoinositide 3-kinase [PI3K(I)]-RNAi-GFP (50 MOI) for 24 h (B), 48 h (C) and 72 h (D), and were then stained with JC-1 (5  $\mu\text{mol/L}$ ) for 30 min.

with the treatment of adenovirus PI3K(I)-RNAi-GFP (50 MOI) (Figure 6).

**Activation of autophagy/lysosomes and impairment of mitochondria with adenovirus PI3K(I)-RNAi-GFP treatment:** We used transmission electron microscopy to identify ultrastructural changes in SGC7901 cells after adenovirus PI3K(I)-RNAi-GFP (50 MOI) treatment. Control cells showed a round shape and contained normal-looking organelles, nucleus, and chromatin (Figure 7), while adenovirus PI3K(I)-RNAi-GFP (50 MOI)-treated cells exhibited the typical signs of autophagy (Figure 4B-D). A number of isolated membranes, possibly derived from ribosome-free endoplasmic reticulum,

were seen. These isolated membranes were elongated and curved to engulf a cytoplasmic fraction and organelles (Figure 7C and D). These membrane structures formed autophagosome traits with double or multi-membranes, and then fused with lysosomes in the formation of autolysosomes. The lysosome staining darkened, indicating the activation of lysosomal enzymes (Figure 7C and D). The loss of organelles and cytoplasm vacuolization were also observed when the incubation time was prolonged (Figure 7C and D).

## DISCUSSION

In the present study, we showed that the RNAi of Class I

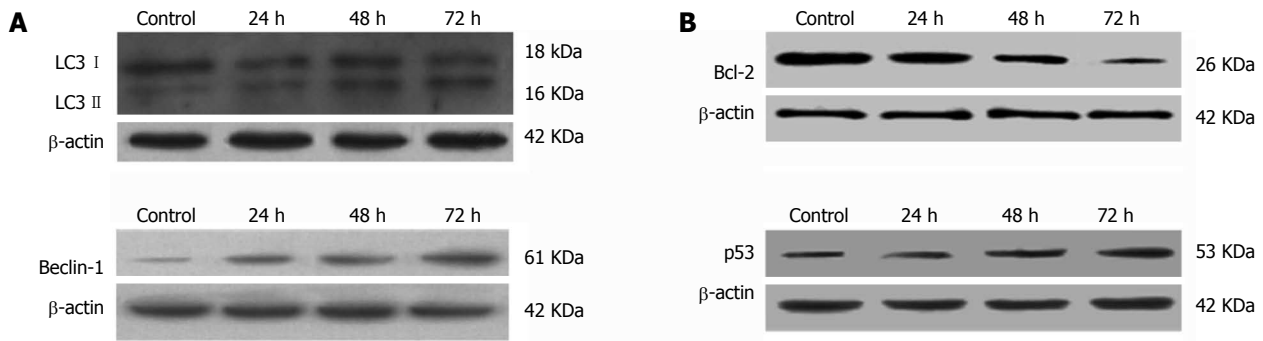


**Figure 6** Effects of adenovirus Class I phosphoinositide 3-kinase-RNA interference-green fluorescent protein on light chain 3 and Beclin-1 protein expression/Bcl-2 and p53 protein expression in SGC7901 cells. A: Effect of adenovirus Class I phosphoinositide 3-kinase [PI3K(I)]-RNA interference-green fluorescent protein (RNAi-GFP) (50 MOI) and adenovirus negative control (NC)-RNAi-GFP on light chain 3 (LC3) and Beclin-1 protein expression. Control: Adenovirus NC-RNAi-GFP. SGC7901 cells were treated with adenovirus PI3K(I)-RNAi-GFP (50 MOI) for 24 to 72 h then harvested for the extraction of total proteins. Adenovirus PI3K(I)-RNAi-GFP up-regulates the expression of LC3 and Beclin protein; B: Adenovirus PI3K(I)-RNAi-GFP (50 MOI) and adenovirus NC-RNAi-GFP on Bcl-2 and p53 protein expression. Control: Adenovirus NC-RNAi-GFP. SGC7901 cells were treated with adenovirus PI3K(I)-RNAi-GFP (50 MOI) for 24 to 72 h then harvested for the extraction of total proteins. Adenovirus PI3K(I)-RNAi-GFP up-regulates the expression of p53 and down-regulates the expression of Bcl-2 protein.

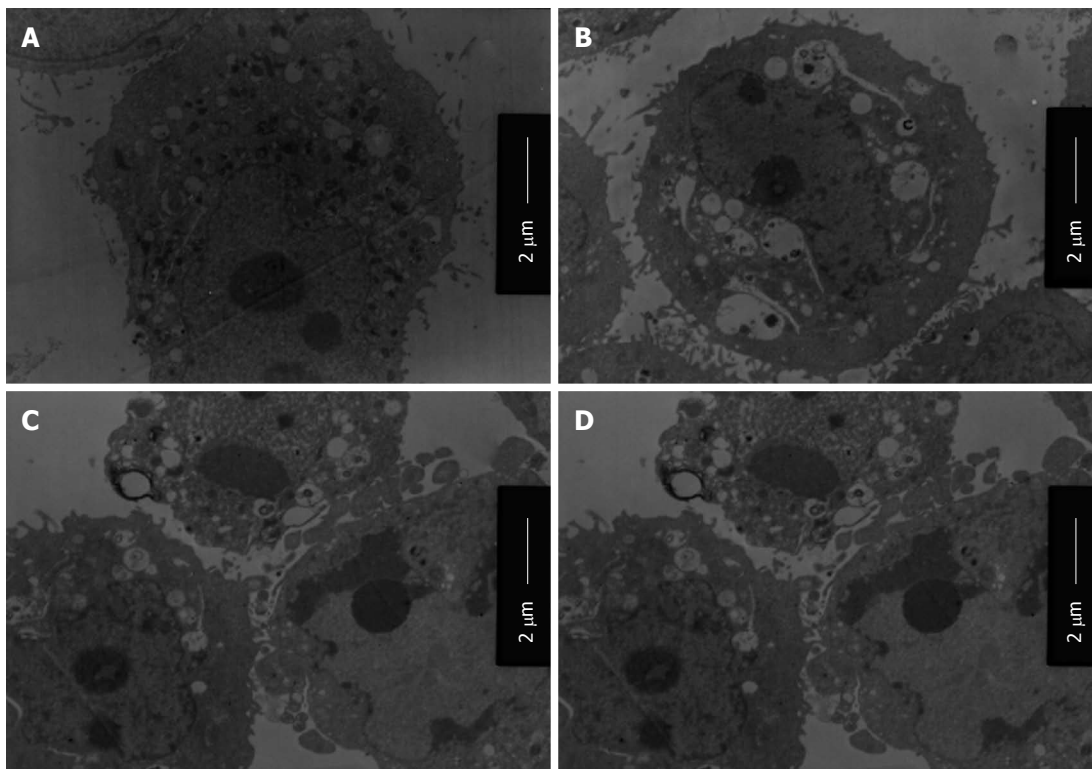


**Figure 7** Ultrastructure of SGC7901 cells undergo autophagy, apoptosis and necrosis after adenovirus Class I phosphoinositide 3-kinase-RNA interference-green fluorescent protein treatment. A: Control: Adenovirus negative control RNA interference-green fluorescent protein (RNAi-GFP); B: Adenovirus Class I phosphoinositide 3-kinase [PI3K(I)]-RNAi-GFP (50 MOI)-treated (24 h); C: Adenovirus PI3K(I)-RNAi-GFP (50 MOI)-treated (48 h); D: Adenovirus PI3K(I)-RNAi-GFP (50 MOI)-treated (72 h).

PI3K reduced viability and induced apoptosis in SGC7901 and MGC803 gastric cancer cells, thus demonstrating the cytotoxic effects of adenovirus PI3K(I)-RNAi-GFP. We also showed that adenovirus PI3K(I)-RNAi-GFP increased the expression of p53, Beclin-1, and LC3, while decreasing the expression of Bcl-2. These findings suggest that RNAi of the Class I PI3K signaling pathway is a potential strategy for managing gastric cancers.

The mitochondria play critical roles in integrating cell death signals. Apoptosis is a cellular process involving the

selective degradation of membranous organelles such as the mitochondria. The mitochondrial permeability transition (MPT) represents an important event in initiating apoptosis. Thus, it is not surprising that apoptosis, and even necrosis, share a common mechanism through induction of the MPT. Observations made in the present study suggest that the mitochondrial  $\Delta\psi$  collapsed after treatment of adenovirus PI3K(I)-RNAi-GFP; thus mitochondria may have initiated an apoptotic pathway.

The tumor suppressor p53 plays a central role in sensing

various genotoxic stresses. The basal levels of p53 were low in SGC7901 gastric cancer cells, and adenovirus PI3K(I)-RNAi-GFP upregulated the expression of p53. Upregulation of p53 after treatment with adenovirus PI3K(I)-RNAi-GFP induced apoptotic cell death. Moll and Zaika have proposed that the induction of apoptotic cell death by p53 occurs *via* both target gene activation and transactivation-independent mechanisms in mitochondria<sup>[14]</sup>. In response to various forms of cellular stress, the levels of p53 increase, and a proportion of p53 rapidly localizes to the mitochondria<sup>[15]</sup>. In the present study, the mitochondrial  $\Delta\psi$  collapse after adenovirus PI3K(I)-RNAi-GFP treatment may have been caused by upregulation of p53. p53 accumulates in the nucleus, where it transactivates a number of proapoptotic target genes<sup>[16]</sup>, and induces apoptotic cell death.

Beclin-1 is monoallelically deleted in human breast and ovarian cancers, where it is expressed at reduced levels<sup>[17,18]</sup>. The present results suggest that autophagy induced by adenovirus PI3K(I)-RNAi-GFP may contribute to anti-tumor effects. We also found that adenovirus PI3K(I)-RNAi-GFP increased the expression of Beclin-1, particularly the production of p53. Bcl-2 and Bcl-xL associate with the evolutionarily-conserved autophagy inducer Beclin-1, a haploinsufficient tumor suppressor<sup>[19]</sup>.

Inhibition may require Bcl-2 localized on the endoplasmic reticulum<sup>[20,21]</sup>; notably, a BH3 domain within Beclin-1 mediates their association<sup>[22]</sup>. In our research, we also found that the expression of Beclin-1 up-regulated with the treatment of adenovirus PI3K(I)-RNAi-GFP and the expression of Bcl-2 decreased. This indicated that autophagy activated and apoptosis induced after adenovirus PI3K(I)-RNAi-GFP treatment decreased the expression of Bcl-2.

All these observations suggest that autophagy and apoptosis activation may have significant contributions to adenovirus PI3K(I)-RNAi-GFP-induced death of SGC7901 and MGC803 cells. Further investigation of upstream signal regulation of autophagy and apoptosis may provide new insights into the mechanisms accommodating or contributing to autophagy and apoptosis, thereby unveiling new strategies for tumor therapy.

## COMMENTS

### Background

The discovery of Class I phosphoinositide 3-kinase (Class I PI3K) revealed a novel role for autophagy in induced cell death, and it is believed to be a crucial modulator in both apoptosis and autophagy. The authors predicted that activation of autophagy by blocking Class I PI3K may contribute to the anti-tumor actions of Class I PI3K inhibitors.

### Research frontiers

The anti-tumor activity of Class I PI3K short hairpin RNA (shRNA) might be related to the induction of apoptosis of tumor cells, but the precise mechanism of its anti-tumor activity is not well understood.

### Innovations and breakthroughs

Blocking Class I PI3K increases the expression of p53 and Beclin-1, and induces apoptotic and autophagic proteins, which contribute to the Class I PI3K inhibitor-induced apoptosis of cancer cells through both apoptotic and autophagic mechanisms. Further investigation of the relationship between autophagy activation and the anti-tumor effects of Class I PI3K inhibitors will unveil new

strategies for tumor therapy.

### Applications

Blocking Class I PI3K increases the expression of p53 and Beclin-1, and induces apoptotic and autophagic proteins, which contribute to Class I PI3K shRNA-induced apoptosis of cancer cells by activating autophagic mechanisms; thereby providing new ideas for tumor treatment.

### Terminology

Autophagy is a general term for the degradation of cytoplasmic components within lysosomes. There are three types of autophagy: macroautophagy, microautophagy, and chaperone-mediated autophagy. The term "autophagy" usually indicates macroautophagy.

### Peer review

The authors examined the effects of Class I PI3K shRNA on the activation of apoptosis and autophagy, and the contribution of autophagy to the cytotoxic effects of Class I PI3K shRNA in gastric cancer cell line SGC7901. The results showed that shRNA Class I PI3K leads to the activation of apoptotic and autophagic pathways, and autophagy activation contributes to Class I PI3K shRNA-induced death of cancer cells.

## REFERENCES

- 1 Crew KD, Neugut AI. Epidemiology of gastric cancer. *World J Gastroenterol* 2006; **12**: 354-362 [PMID: 16489633]
- 2 Cantley LC. The phosphoinositide 3-kinase pathway. *Science* 2002; **296**: 1655-1657 [PMID: 12040186 DOI: 10.1126/science.296.5573.1655]
- 3 Liu LZ, Zhou XD, Qian G, Shi X, Fang J, Jiang BH. AKT1 amplification regulates cisplatin resistance in human lung cancer cells through the mammalian target of rapamycin/p70S6K1 pathway. *Cancer Res* 2007; **67**: 6325-6332 [PMID: 17616691 DOI: 10.1158/0008-5472.CAN-06-4261]
- 4 Faried LS, Faried A, Kanuma T, Aoki H, Sano T, Nakazato T, Tamura T, Kuwano H, Minegishi T. Expression of an activated mammalian target of rapamycin in adenocarcinoma of the cervix: A potential biomarker and molecular target therapy. *Mol Carcinog* 2008; **47**: 446-457 [PMID: 18058806 DOI: 10.1002/mc.20402]
- 5 Yang X, Fraser M, Moll UM, Basak A, Tsang BK. Akt-mediated cisplatin resistance in ovarian cancer: modulation of p53 action on caspase-dependent mitochondrial death pathway. *Cancer Res* 2006; **66**: 3126-3136 [PMID: 16540663 DOI: 10.1158/0008-5472.CAN-05-0425]
- 6 Faried LS, Faried A, Kanuma T, Sano T, Nakazato T, Tamura T, Kuwano H, Minegishi T. Predictive and prognostic role of activated mammalian target of rapamycin in cervical cancer treated with cisplatin-based neoadjuvant chemotherapy. *Oncol Rep* 2006; **16**: 57-63 [PMID: 16786123]
- 7 Hou G, Xue L, Lu Z, Fan T, Tian F, Xue Y. An activated mTOR/p70S6K signaling pathway in esophageal squamous cell carcinoma cell lines and inhibition of the pathway by rapamycin and siRNA against mTOR. *Cancer Lett* 2007; **253**: 236-248 [PMID: 17360108 DOI: 10.1016/j.canlet.2007.01.026]
- 8 Lee S, Choi EJ, Jin C, Kim DH. Activation of PI3K/Akt pathway by PTEN reduction and PIK3CA mRNA amplification contributes to cisplatin resistance in an ovarian cancer cell line. *Gynecol Oncol* 2005; **97**: 26-34 [PMID: 15790433 DOI: 10.1016/j.ygyno.2004.11.051]
- 9 Hennessy BT, Smith DL, Ram PT, Lu Y, Mills GB. Exploiting the PI3K/AKT pathway for cancer drug discovery. *Nat Rev Drug Discov* 2005; **4**: 988-1004 [PMID: 16341064 DOI: 10.1038/nrd1902]
- 10 Biederbick A, Kern HF, Elsässer HP. Monodansylcadaverine (MDC) is a specific in vivo marker for autophagic vacuoles. *Eur J Cell Biol* 1995; **66**: 3-14 [PMID: 7750517]
- 11 Rashid SF, Moore JS, Walker E, Driver PM, Engel J, Edwards CE, Brown G, Uskokovic MR, Campbell MJ. Synergistic growth inhibition of prostate cancer cells by 1 alpha,25 Dihydroxyvitamin D(3) and its 19-nor-hexafluoride analogs in combination with either sodium butyrate or trichostatin A.

- Oncogene* 2001; **20**: 1860-1872 [PMID: 11313934 DOI: 10.1038/sj.onc.1204269]
- 12 **Niemann A**, Takatsuki A, Elsässer HP. The lysosomotropic agent monodansylcadaverine also acts as a solvent polarity probe. *J Histochem Cytochem* 2000; **48**: 251-258 [PMID: 10639491 DOI: 10.1177/002215540004800210]
  - 13 **Yoshimori T**. Autophagy: a regulated bulk degradation process inside cells. *Biochem Biophys Res Commun* 2004; **313**: 453-458 [PMID: 14684184]
  - 14 **Moll UM**, Zaika A. Nuclear and mitochondrial apoptotic pathways of p53. *FEBS Lett* 2001; **493**: 65-69 [PMID: 11286997 DOI: 10.1016/S0014-5793(01)02284-0]
  - 15 **Erster S**, Mihara M, Kim RH, Petrenko O, Moll UM. In vivo mitochondrial p53 translocation triggers a rapid first wave of cell death in response to DNA damage that can precede p53 target gene activation. *Mol Cell Biol* 2004; **24**: 6728-6741 [PMID: 15254240 DOI: 10.1128/MCB.24.15.6728-6741.2004]
  - 16 **Crighton D**, Ryan KM. Splicing DNA-damage responses to tumour cell death. *Biochim Biophys Acta* 2004; **1705**: 3-15 [PMID: 15585169 DOI: 10.1142/S1363246904001614]
  - 17 **Lum JJ**, DeBerardinis RJ, Thompson CB. Autophagy in metazoans: cell survival in the land of plenty. *Nat Rev Mol Cell Biol* 2005; **6**: 439-448 [PMID: 15928708 DOI: 10.1038/nrm1660]
  - 18 **Aita VM**, Liang XH, Murty VV, Pincus DL, Yu W, Cayanis E, Kalachikov S, Gilliam TC, Levine B. Cloning and genomic organization of beclin 1, a candidate tumor suppressor gene on chromosome 17q21. *Genomics* 1999; **59**: 59-65 [PMID: 10395800 DOI: 10.1006/geno.1999.5851]
  - 19 **Qu X**, Yu J, Bhagat G, Furuya N, Hibshoosh H, Troxel A, Rosen J, Eskelinen EL, Mizushima N, Ohsumi Y, Cattoretti G, Levine B. Promotion of tumorigenesis by heterozygous disruption of the beclin 1 autophagy gene. *J Clin Invest* 2003; **112**: 1809-1820 [PMID: 14638851 DOI: 10.1172/JCI200320039]
  - 20 **Pattingre S**, Tassa A, Qu X, Garuti R, Liang XH, Mizushima N, Packer M, Schneider MD, Levine B. Bcl-2 antiapoptotic proteins inhibit Beclin 1-dependent autophagy. *Cell* 2005; **122**: 927-939 [PMID: 16179260 DOI: 10.1016/j.cell.2005.07.002]
  - 21 **Høyer-Hansen M**, Bastholm L, Szyniarowski P, Campanella M, Szabadkai G, Farkas T, Bianchi K, Fehrenbacher N, Elling F, Rizzuto R, Mathiasen IS, Jäättelä M. Control of macroautophagy by calcium, calmodulin-dependent kinase kinase-beta, and Bcl-2. *Mol Cell* 2007; **25**: 193-205 [PMID: 17244528 DOI: 10.1016/j.molcel.2006.12.009]
  - 22 **Oberstein A**, Jeffrey PD, Shi Y. Crystal structure of the Bcl-XL-Beclin 1 peptide complex: Beclin 1 is a novel BH3-only protein. *J Biol Chem* 2007; **282**: 13123-13132 [PMID: 17337444 DOI: 10.1074/jbc.M700492200]

**P- Reviewer** Shibata T **S- Editor** Gou SX  
**L- Editor** Rutherford A **E- Editor** Zhang DN

